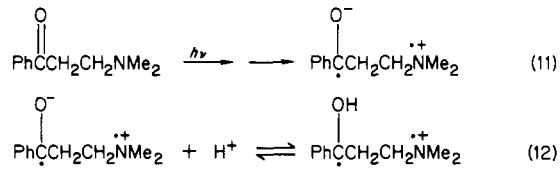

number of bonds away from the acidic OH as in the present case, is some 1.28 pK units more acidic than the isoelectronic uncharged butyric acid.[19] Alternatively, intramolecular proton transfer to form one of the possible neutral ketyl-aminoalkyl biradicals might precede the electron-transfer measurement on which the reported pK_a is predicted. While the pK_a of such nonzwitterionic biradicals would indeed be near 10, this explanation would suggest more photolability than is the case.[18] We regard the pK_a of this biradical as anomalously high, by at least 1 pH unit, and deserving of further study.

The lifetime of the basic form B^- (62 ns) is a factor of 2 shorter than that of the neutral A (125 ns). The ratio is similar to that reported by Encinas and Scaiano[18] for the biradical from β-dimethylaminopropiophenone. Why Norrish II biradicals should behave this way is not clear. Small and Scaiano[5] have shown that the lifetime of Norrish II biradicals increases with increasing basicity of the solvent molecules. Assuming this to result from hydrogen bonding, i.e., partial loss of the acidic hydrogen, one would expect that complete deprotonation would increase the biradical lifetime still further, which is opposite to the present observation.

The explanation more recently suggested by Scaiano[2] for the solvent effect, that H-bonding to solvent creates a bulky terminus which causes an increase in population of a longer-lived *anti* conformation at the expense of a short-lived *gauche*, is also of no help in the present case. We would expect the ionic (basic) form of the biradical B^- to be the more heavily solvated and thus by the same reasoning have the higher fraction of *anti* conformation. Again, this suggests the longer lifetime for B^-, still contrary to observation. In any case, for one clear example, *gauche* and *anti* conformations of a Norrish II biradical have similar lifetimes.[20] Consequently, conformational arguments need not necessarily even apply to all Norrish II biradicals.

Ruling out reasonable explanations which do not fit is, unfortunately, easier than deriving convincing ones which do. At present, our only potentially useful thought is to consider the effect as a polar effect. In that connection, we note that Norrish II biradical lifetimes are, in most of the few cases so far studied, shortened by electron donating polar groups.[4] The O^- group is clearly a better donor than the OH group and the observation thus in this regard consistent with precedent. However, we have more recently noted a case in which the opposite is true.[21] The best generalization we can now make is apparently that these biradical lifetimes are determined by several subtle and delicately balanced factors, with their intersystem crossing possibly subject to more than one electronic mechanism.

Acknowledgment. This work was supported by NSF Grant CHE8213637 and partially (fellowship to D.E.M.) by Robert A. Welch Foundation Grant AT-532. The Center for Fast Kinetic Research at The University of Texas at Austin, at which all flash kinetic work was performed, is supported by NIH Grant RR-00886 from the Biotechnology Branch of the Division of Research Resources and by The University of Texas at Austin. Assistance of Dr. Steven Atherton is gratefully acknowledged. S.N.D. thanks the authorities of Kurukshetra University (Kurukshetra, India) for granting study leave.

Registry No. A, 80326-04-1; K, 5407-91-0.

(19) Edsall, J. T.; Wyman, J. "Biophysical Chemistry"; Academic Press: New York, 1958; Vol. 1, pp 452-3 and 458.

(20) Caldwell, R. A.; Dhawan, S. N.; Majima, T. *J. Am. Chem. Soc.* **1984**, *106*, 6454.

(21) Caldwell, R. A.; Moore, D. E., unpublished.

Conformation, Bonding, and Flexibility in Short-Chain Linear Phosphazenes

Harry R. Allcock,* Norris M. Tollefson, Robert A. Arcus, and Robert R. Whittle

Contribution from the Department of Chemistry, The Pennsylvania State University, University Park, Pennsylvania 16802. *Received November 9, 1984*

Abstract: A number of linear, short-chain phosphazenes have been prepared as structural models for three classes of phosphazene linear high polymers. X-ray diffraction results from studies of $OP(Cl_2)NPCl_3$ (**7**), $OP(Cl_2)NP(Cl_2)NPCl_3$ (**10**), $[Cl_3PNP(Cl_2)NP(Cl_2)NPCl_3]^+PCl_6^-$ (**14**), $OP(OPh)_2NP(OPh)_3$ (**8**), $OP(NHPh)_2NP(NHPh)_3$ (**9**), and $OP(NHPh)_2NP(NHPh)_2NP(NHPh)_3$ (**12**) suggest different values for the bond angles and bond lengths than have been used in the past in structural studies of the high polymers. The P-N bond lengths in the short-chain species differ by 0.07 Å or less within each molecule, and planar skeletal conformations are preferred, especially cis-trans planar. The evidence suggests that, although the molecules are stabilized by electron delocalization, the conformations originate from intramolecular nonbonding interactions. The short phosphazene chains stack in the crystal lattice in a parallel arrangement analogous to that expected in polymer microcrystallites. Comparisons between the ^{31}P NMR shifts of the short chain species and the corresponding high polymers revealed a close similarity between the electronic and structural environments of the middle units in the short chain species and in the repeating units of the high polymers.

The availability of new high polymer systems based on a polyphosphazene backbone provides an opportunity for the exploration of the influence of inorganic elements and different side groups on the conformations and bond torsional mobility of macromolecular chains. Typical high polymeric phosphazene structures are shown in **1**-**3**.[1-4] Those species with organic side groups are derived from poly(dihalophosphazenes), such as **1**, by nucleophilic-type substitution reactions.[5,6]

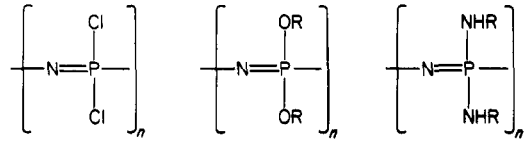

1 **2** **3**

($n \simeq 15\,000$; R=alkyl or aryl)

(1) (a) Allcock, H. R. In "Rings, Clusters, and Polymers of the Main Group Elements"; Cowley, A. H., Ed.; American Chemical Society: Washington, DC, 1983; ACS Symp. Ser. 232, p 49. (b) Allcock, H. R. *Chem. Eng. News* **1985**, *63*, 22.

0002-7863/85/1507-5166$01.50/0

One reason for our interest in these macromolecules is that significant physicochemical differences exist between these polymers and their totally organic counterparts, and also between polyphosphazenes that bear different side groups. Thus, a study of these polymers provides an opportunity to answer questions that are relevant to macromolecular chemistry as a whole.

Information is needed for all types of macromolecules to correlate solid state or solution properties with molecular structure, conformation, and conformational freedom. Much relevant information has been accumulated for organic-type polymers and polysiloxanes but, even here, a serious hurdle is the synthesis and isolation of comparison polymers that have identical main chain structures and identical chain lengths and molecular weight distributions and which differ only in the structure of the side groups. The substitutive mode of synthesis used for the preparation of poly(organophosphazenes) allows this problem to be simplified.[1]

Any attempt to correlate macromolecular structure with physical or chemical properties must be based on a clear understanding of fundamental factors such as bond lengths, bond angles, torsional mobility of bonds, preferred conformations, etc. Unfortunately, such data are difficult to acquire for any macromolecular system. For polyphosphazenes, fiber X-ray diffraction data have been used to propose chain repeat distances and approximate bond lengths, bond angles, and conformations.[1,7,8] Conformational energy calculations based on molecular mechanics-type techniques have been employed to probe conformational preferences and chain flexibilities.[9,10] But good primary structural information has proved hard to obtain.

Until now, emphasis has been placed on the acquisition of X-ray structural data from cyclic trimeric model systems such as **4–6**, or from the corresponding cyclic tetramers.[11] This approach is

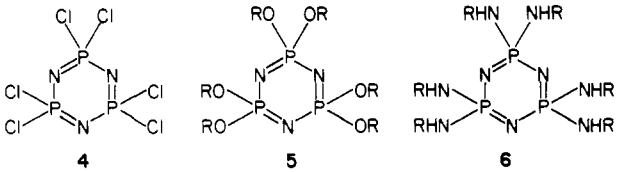

4 **5** **6**

only partly valid because the constraints of a cyclic molecule are bound to affect bond angles and bond lengths, and this will disguise differences in conformational freedom or conformational preference.

In this paper, we describe a sounder approach to solving this problem. We have synthesized a number of short-chain analogues of macromolecular phosphazenes and have examined their structures and conformations by X-ray diffraction methods. In addition, we have probed the electronic and structural environments within the short chains by means of ^{31}P NMR spectroscopy. This has allowed us to identify weaknesses in data derived from cyclic model compounds and has afforded valuable correlations between the short-chain and macromolecular systems.

Results and Discussion

Syntheses. Species **7–16** were the main compounds used in this study. The following methods were employed for their synthesis. (a) The phosphorylphosphazene **7**, was prepared from PCl_5 and

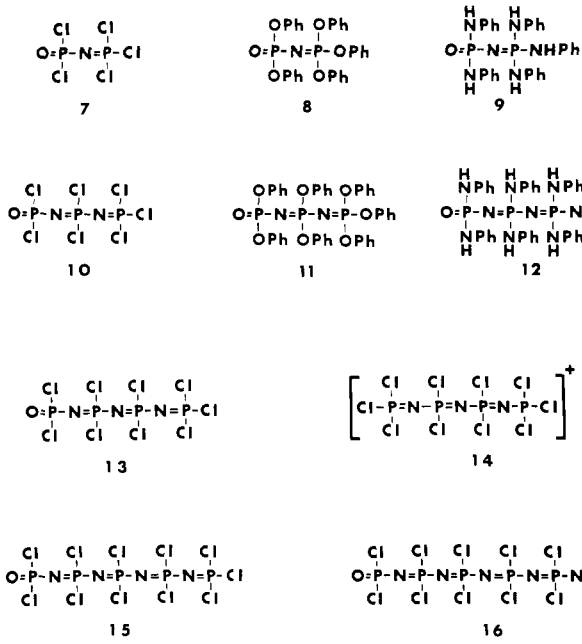

7 **8** **9**

10 **11** **12**

13 **14**

15 **16**

$(NH_4)_2SO_4$.[12] Compound **7** was also used as a starting material for the preparation of longer chain species. (b) Compound **10** was prepared via a chain-building method developed by Riesel,[13] through the interaction of **7** with hexamethyldisilazane, followed by treatment with PCl_5. This method could not be used for the less volatile longer chain species, such as **13**. (c) Compound **13** was, therefore, prepared by the interaction of SO_2 with $[Cl_3PNP(Cl)_2\text{-}N\text{-}P(Cl_2)\text{-}N\text{-}PCl_3]^+PCl_6^-$ or Cl^-.[14] The volatile side products, $OPCl_3$ and $OSCl_2$, were removed in vacuo to yield relatively pure (>90%) samples of **13**. (d) The longer chain species, such as **15** and **16**, were synthesized by the reaction of $OPCl_3$ or **7** with hexamethyldisilazane, followed by treatment with $[Cl_3P{=}N{-}PCl_2{=}N{-}PCl_2{=}N{-}PCl_3]^+PCl_6^-$ or Cl^-. (e) An alternative method used for the preparation of **10** was via the reaction of $[Cl_3P{=}N{-}PCl_2{=}N{-}PCl_3]^+PCl_6^-$ with SO_2.[15] Compounds **7**, **10**, and **13** have been reported earlier.[13-15] These interactions are summarized in Schemes I and II.

The organic derivatives, **8**, **9**, **11**, and **12**, were obtained by treatment of the appropriate linear chlorophosphazenes with excess sodium phenoxide or aniline. Of these, only compound **9** appears to have been synthesized previously.[13]

Of the compounds isolated, species **7**, **8**, **9**, **10**, **12**, and **14** were induced to form single crystals appropriate for X-ray diffraction analysis. The others were oils, even after prolonged manipulation at low temperatures. Hence, compounds **11**, **13**, **15**, and **16** were studied only by ^{31}P NMR techniques.

X-ray Structure Results. The objectives in this part of the work were to obtain the following: (1) molecular structural data, such as bond lengths, bond angles, torsional angles, and information about planar or twisted chain conformations; (2) evidence about the electronic structures, especially π-bonding, from skeletal bond length equalities or inequalities, bond angles, etc.; and (3) information about intra- and intermolecular nonbonding distances that might explain conformational preferences or crystalline packing arrangements related to the microcrystalline structure in the macromolecular analogues.

(a) $OP(Cl_2)NPCl_3$ (7). The X-ray data collected at 25 °C revealed an extremely high degree of thermal motion in the bridging nitrogen atom. This can be attributed to the fact that,

(2) Allcock, H. R. *Makromol. Chem.* **1981**, *Suppl. 4*, 3.
(3) Allcock, H. R. "Phosphorus-Nitrogen Compounds"; Academic Press: New York, 1972.
(4) Singler, R. E.; Schneider, N. S.; Hagnauer, G. L. *Polym. Eng. Sci.* **1975**, *15*, 322. Singler, R. E.; Hagnauer, G. L. In "Organometallic Polymers"; Carraher, C. E., Sheats, J. E., Pittman, C. U., Eds.; Academic Press: New York, 1978.
(5) (a) Allcock, H. R.; Kugel, R. L. *J. Am. Chem. Soc.* **1965**, *87*, 4216. (b) Allcock, H. R.; Kugel, R. L.; Valan, K. *Inorg. Chem.* **1966**, *5*, 1709.
(6) Allcock, H. R.; Kugel, R. L. *Inorg. Chem.* **1966**, *5*, 1716.
(7) Allcock, H. R.; Kugel, R. L.; Stroh, E. G. *Inorg. Chem.* **1972**, *11*, 1120.
(8) Allcock, H. R.; Arcus, R. A. *Macromolecules* **1979**, *12*, 1130.
(9) Allcock, H. R.; Allen, R. W.; Meister, J. J. *Macromolecules* **1976**, *9*, 950.
(10) Allen, R. W.; Allcock, H. R. *Macromolecules* **1976**, *9*, 956.
(11) Allcock, H. R. *Acc. Chem. Res.* **1979**, *12*, 351.
(12) Emsley, J.; Moore, J.; Udy, P. B. *J. Chem. Soc. A* **1971**, 2863.
(13) Riesel, L.; Somiesi, R. *Z. Anorg. Allg. Chem.* **1975**, *411*, 148.
(14) $N_3P_4Cl_{10}^+Cl^-$ was prepared from $(NPCl_2)_3$ and PCl_5. (a) Fluck, E. *Z. Anorg. Allg. Chem.* **1962**, 315, 191. (b) Moran, E. F. *J. Inorg. Nucl. Chem.* **1968**, *30*, 1405.
(15) (a) Becke-Goehring, M.; Lehr, W. *Chem. Ber.* **1961**, *94*, 1591; *Z. Anorg. Allg. Chem.* **1963**, 325, 286. (b) Becke-Goehring, M.; Mann, T.; Euler, H. D. *Chem. Ber.* **1961**, *94*, 193.

Scheme I

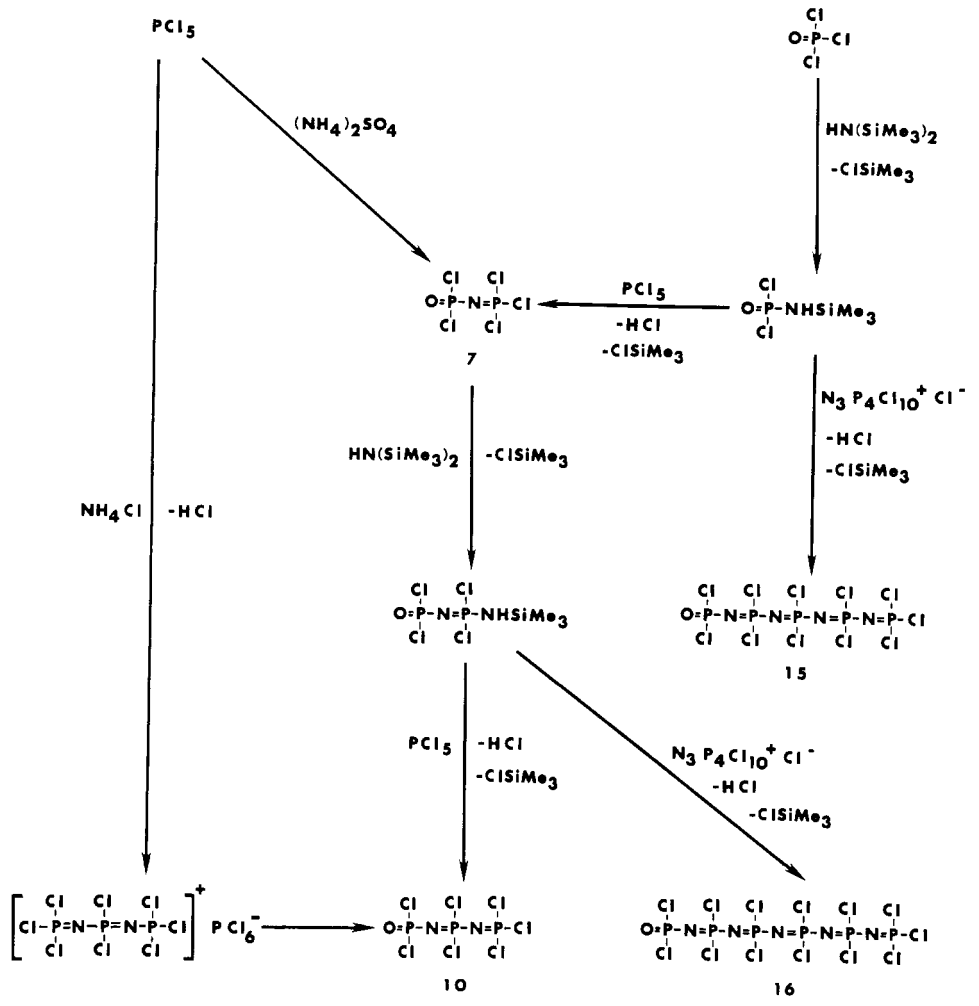

Scheme II

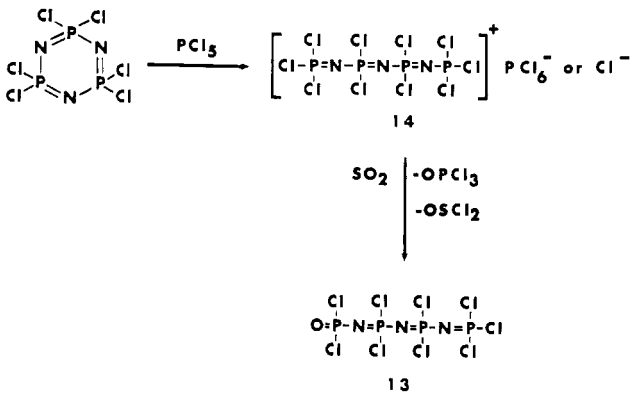

at 25 °C, the crystal is only a few degrees below its melting point. However, this discrepancy remained as positional disorder even when a data set was collected with the crystal cooled to −50 °C. Thus, some uncertainty exists about the exact location of the nitrogen atom and this, in turn, reduced the reliability of the P–N bond lengths and P–N–P angles. When cooled below −50 °C, the crystal undergoes a transition which generates a slightly different packing arrangement.

On the basis of the −50 °C crystal data, the average P···P distance is 2.95 Å, and this is typical of cyclophosphazenes and other linear, short-chain phosphazenes. An isotropic treatment of the nitrogen atoms (again based on the low-temperature data set) suggested an "average" P–N–P bond angle of 144–148°. The atom identification scheme and molecular structure are shown in Figure 1 for the two unique molecules in the unit cell. Other

Table I. Bond Lengths (Å) and Bond Angles (deg) for OP_2NCl_5 (7) (−50 °C)

A		B	
P(1)–Cl(1)	1.980 (4)	P(1)–Cl(1)	1.974 (5)
P(1)–Cl(2)	1.979 (4)	P(1)–Cl(2)	1.940 (5)
P(1)–O	1.453 (8)	P(1)–O	1.398 (10)
P(1)–N	1.580 (8)	P(1)–N	1.53 (2)
P(2)–Cl(3)	1.942 (4)	P(2)–Cl(3)	1.937 (4)
P(2)–Cl(4)	1.950 (4)	P(2)–Cl(4)	1.940 (4)
P(2)–Cl(5)	1.949 (4)	P(2)–Cl(5)	1.930 (5)
P(2)–N	1.519 (8)	P(2)–N	1.54 (2)
Cl(1)–P(1)–Cl(2)	102.6 (2)	Cl(1)–P(1)–Cl(2)	103.4 (2)
Cl(1)–P(1)–O	110.5 (3)	Cl(1)–P(1)–O	111.8 (5)
Cl(1)–P(1)–N	108.7 (4)	Cl(1)–P(1)–N	109.6 (7)
Cl(2)–P(1)–O	111.3 (4)	Cl(2)–P(1)–O	113.1 (5)
Cl(2)–P(1)–N	108.6 (4)	Cl(2)–P(1)–N	112.4 (7)
O–P(1)–N	114.5 (4)	O–P(1)–N	106.7 (8)
Cl(3)–P(2)–Cl(4)	103.7 (2)	Cl(3)–P(2)–Cl(4)	106.2 (2)
Cl(3)–P(2)–Cl(5)	106.1 (2)	Cl(3)–P(2)–Cl(5)	106.2 (2)
Cl(3)–P(2)–N	116.9 (3)	Cl(3)–P(2)–N	119.6 (7)
Cl(4)–P(2)–Cl(5)	104.4 (2)	Cl(4)–P(2)–Cl(5)	105.9 (2)
Cl(4)–P(2)–N	108.8 (4)	Cl(4)–P(2)–N	117.7 (7)
Cl(5)–P(2)–N	115.8 (4)	Cl(5)–P(2)–N	99.5 (7)
P(1)–N–P(2)	144.5 (6)	P(1)–N–P(2)	148.0 (1)

structural parameters are listed in Table I with the positional parameters for the low-temperature structure summarized in Table II. The corresponding values for the 25 °C structure are given in the Supplementary Material.

The most important result from this structure solution is the mode of packing of the molecules in the unit cell (Figure 1). The

Table II. Fractional Atomic Positional Parameters for OP_2NCl_5 (**7**) (−50 °C)

	A				B		
	x	*y*	*z*		*x*	*y*	*z*
P(1)	0.0784 (3)	0.2534 (1)	0.4675 (2)	P(1)	0.1731 (3)	0.5112 (1)	0.2437 (2)
P(2)	0.4311 (3)	0.2833 (1)	0.4486 (2)	P(2)	−0.1942 (3)	0.4993 (2)	0.2387 (3)
Cl(1)	−0.0339 (4)	0.2697 (2)	0.2975 (3)	Cl(1)	0.1879 (5)	0.6008 (2)	0.1670 (4)
Cl(2)	0.0308 (4)	0.3391 (2)	0.5469 (3)	Cl(2)	0.1995 (7)	0.4464 (2)	0.1200 (4)
Cl(3)	0.4288 (5)	0.2999 (2)	0.2802 (3)	Cl(3)	−0.2946 (5)	0.4222 (2)	0.1425 (3)
Cl(4)	0.6300 (4)	0.2252 (2)	0.5015 (4)	Cl(4)	−0.3167 (5)	0.5796 (2)	0.1670 (3)
Cl(5)	0.4941 (5)	0.3698 (2)	0.5310 (3)	Cl(5)	−0.2517 (5)	0.4885 (2)	0.3937 (3)
O	0.0030 (8)	0.1948 (4)	0.5147 (7)	O	0.297 (2)	0.5040 (6)	0.3495 (8)
N	0.2766 (9)	0.2477 (4)	0.4771 (7)	N	0.001 (2)	0.5045 (9)	0.279 (2)

packing arrangement shown is for the −50 °C form. The asymmetric portion of the unit cell consists of two molecules, A and B. The molecules pack in sheets of molecules A, alternating with sheets of molecules B. The layers are staggered in such a way that the chlorine atoms in one sheet are oriented toward the nitrogen atoms in the molecules of the adjacent layer. The chain directions of molecules A and B roughly parallel the *a* axis of the unit cell.

(b) $OP(Cl_2)NP(Cl_2)NPCl_3$ (10). The structure of **10** provided a considerable amount of useful information. The overall conformation and the atom designations are shown in Figure 1. A significant feature is the planarity of the phosphazene skeleton ($\chi^2 = 68$, N(1) deviates from the plane of P(1)–N(1)–P(2)–N(2)–P(3) by only 0.12 Å), and the existence of what, in the high polymer, would correspond to a cis–trans planar conformation.

Why does the molecule adopt a planar conformation of this type? Is it a consequence of π-bonding effects in the skeleton, or can it be explained by inter- or intramolecular nonbonding effects? We believe that intramolecular nonbonding influences explain the data adequately. Consider the schematic view of the molecule shown in structure **17** and its relationship to **10** in Figure 1.

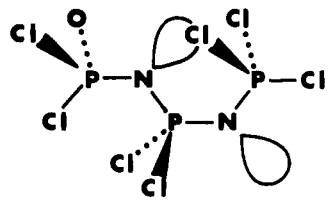

17

The intramolecular distances between N(1) and Cl(5) or Cl(6) are 3.51 or 3.61 Å, respectively. This is slightly longer than the calculated sum of the van der Waals radii (3.3 Å). However, twisting of bond N(2)–P(3) would reduce this distance and presumably generate repulsions. If the lone-pair orbital on N(1) is taken into account (structure **17**), the need for the molecule to maintain a planar conformation becomes even more compelling. Thus, we see no reason to invoke π-bonding to explain the conformational preference. Indeed, if the bonding is of the d_π–p_π type, with an "island" delocalization character of the type proposed by Dewar, Lucken, and Whitehead 25 years ago,[16] the π-bonding *should* have no influence on the conformation. A nitrogen $2p_z$ orbital would have the opportunity to interact with the lobes of any of five accessible, diffuse d orbitals on the phosphorus.

What is especially interesting about this structure is that the "steric" influence of the side groups is evident even when the side groups are as small as chlorine atoms. Thus, even more striking effects might be expected when the side groups are larger.

The details of the structure of **10** are also interesting (Tables III and IV). Three of the bond lengths [P(1)–N(1), N(1)–P(2), and P(2)–N(2)] are equal (av. 1.55 Å), and only the terminal bond N(2)–P(3) is slightly longer at 1.59 Å. Thus, no separation into discrete single and double P–N bonds was detected. The bond

(16) Dewar, M. J. S.; Lucken, E. A. C.; Whitehead, M. A. *J. Chem. Soc. London* **1960**, 2423.

Table III. Bond Lengths (Å) and Bond Angles (deg) for $OP_3N_2Cl_7$ (**10**)

P(1)–N(1)	1.546 (9)	P(1)–Cl(2)	1.989 (4)
P(2)–N(1)	1.543 (9)	P(2)–Cl(3)	1.973 (4)
P(2)–N(2)	1.537 (9)	P(2)–Cl(4)	1.988 (4)
P(3)–N(2)	1.589 (9)	P(3)–Cl(5)	1.948 (4)
P(1)–O	1.456 (7)	P(3)–Cl(6)	1.966 (4)
P(1)–Cl(1)	1.973 (5)	P(3)–Cl(7)	1.944 (4)
P(1)–N(1)–P(2)	144.4 (6)	Cl(3)–P(2)–N(2)	107.1 (4)
P(2)–N(2)–P(3)	128.7 (6)	Cl(4)–P(2)–N(1)	111.3 (4)
N(1)–P(2)–N(2)	116.8 (5)	Cl(4)–P(2)–N(2)	105.1 (4)
O–P(1)–N(1)	119.1 (5)	Cl(3)–P(2)–Cl(4)	102.3 (2)
Cl(1)–P(1)–N(1)	107.4 (4)	Cl(5)–P(3)–N(2)	115.7 (4)
Cl(2)–P(1)–N(1)	109.4 (4)	Cl(6)–P(3)–N(2)	112.0 (4)
Cl(1)–P(1)–Cl(2)	100.4 (3)	Cl(7)–P(3)–N(2)	110.8 (4)
O–P(1)–Cl(1)	109.6 (4)	Cl(5)–P(3)–Cl(6)	105.5 (2)
O–P(1)–Cl(2)	109.3 (4)	Cl(5)–P(3)–Cl(7)	106.3 (2)
Cl(3)–P(2)–N(1)	112.9 (4)	Cl(6)–P(3)–Cl(7)	105.9 (2)

Table IV. Fractional Positional Parameters for $OP_3N_2Cl_7$ (**10**)

	x	*y*	*z*
P(1)	0.8453 (8)	1.1040 (6)	0.2711 (4)
P(2)	0.6415 (8)	0.7679 (6)	0.1794 (4)
P(3)	0.3876 (8)	0.6876 (5)	0.3461 (4)
N(1)	0.726 (2)	0.934 (2)	0.261 (1)
N(2)	0.485 (2)	0.654 (2)	0.225 (1)
O	0.970 (2)	1.191 (2)	0.373 (1)
Cl(1)	0.623 (1)	1.2420 (8)	0.2407 (6)
Cl(2)	1.037 (1)	1.089 (1)	0.1416 (5)
Cl(3)	0.496 (1)	0.7907 (8)	0.0445 (4)
Cl(4)	0.889 (1)	0.6355 (8)	0.1175 (6)
Cl(5)	0.2330 (9)	0.8847 (6)	0.3975 (4)
Cl(6)	0.6187 (9)	0.7070 (7)	0.4604 (4)
Cl(7)	0.1801 (9)	0.5067 (6)	0.3542 (4)

angles at skeletal nitrogen are unusually wide, 144.4° at N(1) and 128.7° at N(2). These angles are much wider than has been assumed in the past for phosphazene high polymers. They are also wider than those found in cyclic trimeric phosphazenes. This illustrates a weakness in the use of structural data from cyclic trimers for the interpretation of high polymeric structures. Considerable angular flexibility apparently exists in P–N–P bond angles, and this may help to explain the high chain flexibility of poly(dichlorophosphazene).

The organization of the molecules of **10** in the solid is depicted in Figure 1. Some evidence exists from this packing pattern that the conformation adopted by **10** also minimizes Cl···N intermolecular repulsions.

(c) $N_3P_4Cl_{10}^+PCl_6^-$ (14). Crystallographically, the $N_3P_4Cl_{10}^+PCl_6^-$ ion pair occupies a unique position in the unit cell, with a mirror plane bisecting the cation through the central nitrogen and through the anion.

The skeleton of the cation is planar (Figure 1) but, unlike the structure of **10**, the conformation corresponds to a trans–trans planar structure. This geometry may be a consequence of an attempt by the cation to generate as many close contacts as possible with the anion. For example, the interionic distances from N(1) and N(2) to Cl(9) are similar (3.86 and 3.71 Å). The distance between Cl(3) and Cl(9) is 4.10 Å. No evidence was found that

Table V. Bond Lengths (Å) and Bond Angles (deg) for $P_4N_3Cl_{10}^+PCl_6^-$ (**14**)

P(1)–N(1)	1.498 (5)	P(2)–Cl(5)	1.970 (2)
P(2)–N(1)	1.572 (5)	P–Cl(6)	2.146 (3)
P(2)–N(2)	1.527 (3)	P–Cl(7)	2.133 (3)
P(1)–Cl(1)	1.953 (3)	P–Cl(8)	2.093 (3)
P(1)–Cl(2)	1.930 (2)	P–Cl(9)	2.126 (3)
P(1)–Cl(3)	1.937 (3)	P–Cl(10)	2.129 (2)
P(2)–Cl(4)	1.972 (2)		
P(1)–N(1)–P(2)	144.8 (4)	Cl(6)–P–Cl(7)	89.4 (1)
P(2)–N(2)–P(2)	143.1 (5)	Cl(6)–P–Cl(8)	89.8 (1)
N(1)–P(2)–N(2)	110.9 (3)	Cl(6)–P–Cl(9)	178.9 (1)
		Cl(6)–P–Cl(10)	89.12 (8)
Cl(1)–P(1)–N(1)	114.8 (3)	Cl(7)–P–Cl(8)	179.2 (1)
Cl(2)–P(1)–N(1)	115.9 (3)	Cl(7)–P–Cl(9)	89.5 (1)
Cl(3)–P(1)–N(1)	109.1 (2)	Cl(7)–P–Cl(10)	88.53 (9)
Cl(1)–P(1)–Cl(2)	106.2 (1)	Cl(8)–P–Cl(9)	91.3 (1)
Cl(1)–P(1)–Cl(3)	105.0 (1)	Cl(8)–P–Cl(10)	91.46 (9)
Cl(2)–P(1)–Cl(3)	105.0 (1)	Cl(9)–P–Cl(10)	90.85 (8)
Cl(4)–P(2)–N(1)	110.0 (2)	Cl(10)–P–Cl(10)	176.6 (2)
Cl(5)–P(2)–N(1)	109.1 (0)		
Cl(4)–P(2)–N(2)	112.3 (3)		
Cl(5)–P(2)–N(2)	111.1 (3)		
Cl(4)–P(2)–Cl(5)	103.2 (1)		

Table VI. Fractional Atomic Positional Parameters for $P_4N_3Cl_{10}^+PCl_6^-$ (**14**)

	x	*y*	*z*
P(1)	−0.0919 (3)	−0.1319 (2)	0.4683 (2)
P(2)	0.0403 (3)	−0.1803 (2)	0.6450 (2)
N(1)	−0.0589 (8)	−0.1436 (5)	0.5728 (6)
N(2)	0.002 (1)	−0.1644 (7)	0.750
Cl(1)	0.3015 (4)	−0.0702 (3)	0.3956 (3)
Cl(2)	−0.1186 (6)	−0.2237 (2)	0.3933 (3)
Cl(3)	−0.2527 (3)	−0.0764 (2)	0.4595 (3)
Cl(4)	0.0577 (4)	−0.2907 (2)	0.6184 (3)
Cl(5)	0.2131 (3)	−0.1404 (3)	0.6166 (3)
P	0.0814 (3)	−0.5558 (2)	0.750
Cl(6)	−0.0623 (3)	−0.6439 (2)	0.750
Cl(7)	0.2270 (4)	−0.6417 (2)	0.750
Cl(8)	−0.0635 (4)	−0.4727 (3)	0.750
Cl(9)	0.2265 (4)	−0.4702 (2)	0.750
Cl(10)	0.0829 (3)	−0.5593 (2)	0.9042 (2)

the conformation was due to interactions between adjacent $N_3P_4Cl_{10}^+$ units.

Although the P–N bond lengths in **14** are different (1.50 and 1.57 Å, average = 1.53 Å), they are not sufficiently different to suggest a separation into distinct double and single bonds. However, it is clear that the cationic charge has a marked effect on the skeletal structure.

The P–Cl bond distances within the cation are of two types. In the end groups, the average distance is 1.94 Å. In the middle unit, the P–Cl distances are close to 1.97 Å. These values are similar to those found for **7** and **10**. The central N–P–N bond angle in the cation is 110.9°, which is narrower than the value found for other chlorophosphazenes, linear or cyclic. This may reflect the presence of the cationic charge. The P–N–P bond angles at N(1) and N(2) are 144.8° and 143.1°, respectively, and these values further confirm the general wideness of such angles when the system is not constrained by a ring.

The packing of the anions and cations in the unit cell (Figure 1) allows two cationic chains to lie in parallel but opposed orientations, flanked above and below by two anions. The other nearby cations are colinear with the first set, but with the skeletal plane tilted roughly 115° to those of the first set. The structural parameters are summarized in Tables V and VI.

(d) $OP(OPh)_2NP(OPh)_3$ (8). Unlike the situation found for compound **7**, the X-ray structure of **8** was well-defined, with normal thermal elipsoids found for all three skeletal atoms (Figure 2). Within the unit cell, the molecules of **8** are aligned roughly parallel to the *a* axis of the cell while in the *b* direction the molecules pack in staggered layers (Figure 2). The sterically large phenoxy residues appear to exert a major influence on the molecular conformation and on the crystal packing arrangement. The disposition of the side groups in **8** is probably unrelated to the situation in the linear high polymer; $[NP(OPh)_2]_n$, because P(2) bears three phenoxy groups. Thus, the conformation of **8** is determined by the need for the molecule to avoid close contacts between phenoxy groups on the different phosphorus atoms and by a preference for a conformation that allows the terminal oxygen on one phosphorus to experience a long-range attraction for one of the phenoxy units on the other phosphorus.

Table VII. Selected Bond Lengths (Å) and Bond Angles (deg) for $OP_2N(OC_6H_5)_5$ (**8**)

P(1)–N	1.596 (4)	O(1)–C(11)	1.386 (6)
P(1)–O	1.456 (4)	O(2)–C(21)	1.394 (7)
P(1)–O(1)	1.593 (3)	O(3)–C(31)	1.412 (5)
P(1)–O(2)	1.587 (3)	O(4)–C(41)	1.415 (6)
P(2)–N	1.525 (4)	O(5)–C(51)	1.403 (6)
P(2)–O(3)	1.555 (3)		
P(2)–O(4)	1.567 (3)		
P(2)–O(5)	1.566 (3)		
P(1)–N–P(2)	133.9 (3)	P(1)–O(1)–C(11)	126.4 (3)
N–P(1)–O	119.3 (2)	P(1)–O(2)–C(21)	124.5 (3)
N–P(1)–O(1)	103.5 (2)	P(2)–O(3)–C(31)	128.0 (3)
N–P(1)–O(2)	106.2 (3)	P(2)–O(4)–C(41)	122.2 (3)
O–P(1)–O(1)	113.5 (2)	P(2)–O(5)–C(51)	123.7 (3)
O–P(1)–O(2)	108.6 (2)		
O(1)–P(1)–O(2)	104.6 (2)		
N–P(2)–O(3)	111.4 (2)		
N–P(2)–O(4)	119.8 (2)		
N–P(2)–O(5)	111.0 (2)		
O(3)–P(2)–O(4)	101.6 (2)		
O(3)–P(2)–O(5)	108.8 (2)		
O(4)–P(2)–O(5)	103.4 (2)		

The structural parameters are summarized in Tables VII and VIII. The P–N bond lengths are similar but unequal. The distance of P(1)–N is 1.60 Å and that of P(2)–N is 1.53 Å. One possible explanation for the inequality is that, compared to **10** and **14**, the lower degree of electron withdrawal by phenoxy reduces the π-overlap character of the phosphorus *d* orbitals, thus reducing π delocalization. However, it should be noted that the distance of P(1)–N is still considerably shorter than the $\simeq$1.68 Å single bond value found in organocyclophosphazanes[3] and the 1.78-Å value quoted for sodium phosphoramidate.[17] Thus, the P–N bonds in **8** can still be viewed as delocalized d_π–p_π linkages.

The P–N–P angle is 134°, again much wider than would have been predicted from the structures of phosphazene cyclic trimers. The P=O bond distance is 1.46 Å. This is similar to values found for other phosphorylphosphazenes but, as expected, is significantly shorter than the other P–O bonds in **8**, which have an average value of 1.57 Å.

(e) $OP(NHPh)_2NP(NHPh)_3$ (9). Compound **9** crystallized from acetonitrile with solvent molecules included within the lattice. However, no substantial interaction could be detected between the host and guest molecules that might indicate an alteration of the host molecular structure by the clathration process.

The skeleton (including the terminal oxygen) atom is planar. The overall atomic arrangement in **9** is shown in Figure 2, and the structural details are summarized in Tables IX and X. Perhaps the most interesting feature of this structure is the manner in which the anilino side groups are oriented. One terminal anilino residue attached through N(50) is approximately coplanar with the phosphazene skeleton. The remaining side groups are extended on either side of the skeletal plane in near parallel arrays. Each pair of aromatic residues on a given side of the plane is oriented to minimize steric interactions. For example, the dihedral angle between planes –N(20)Ph and N(30)Ph is only 9.9°, and the angle between planes –N(10)Ph and N(40)Ph is 32.7°. Moreover, the –N(20)Ph and –N(30)Ph units on different molecules are roughly parallel.

(17) Hobbs, E.; Corbridge, D. E. C.; Raistrick, B. *Acta Crystallogr.* **1953**, *6*, 621.

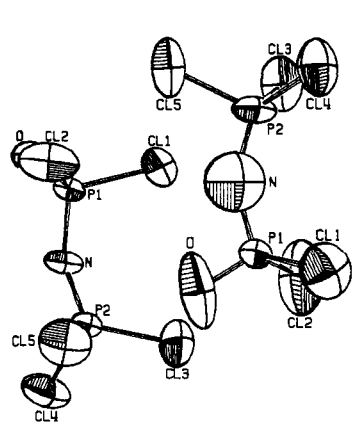

7

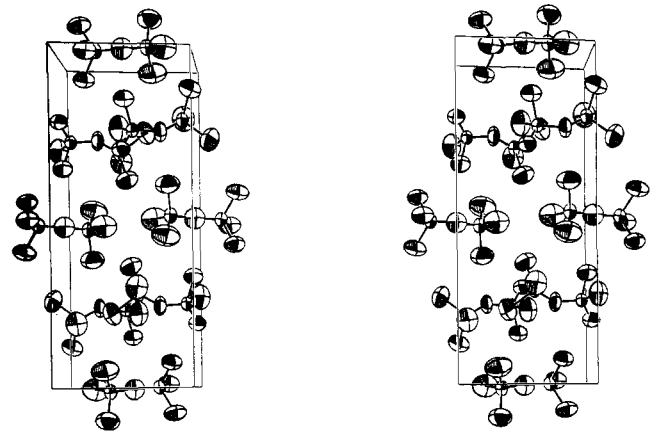

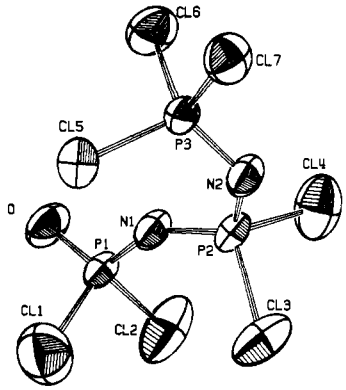

10

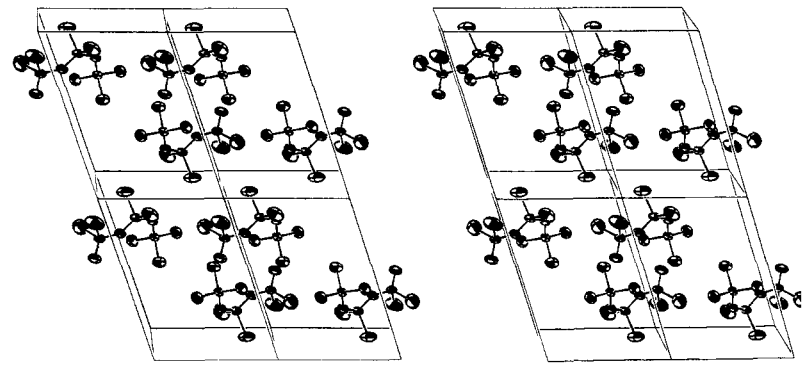

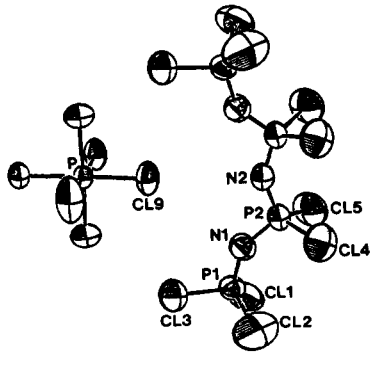

14

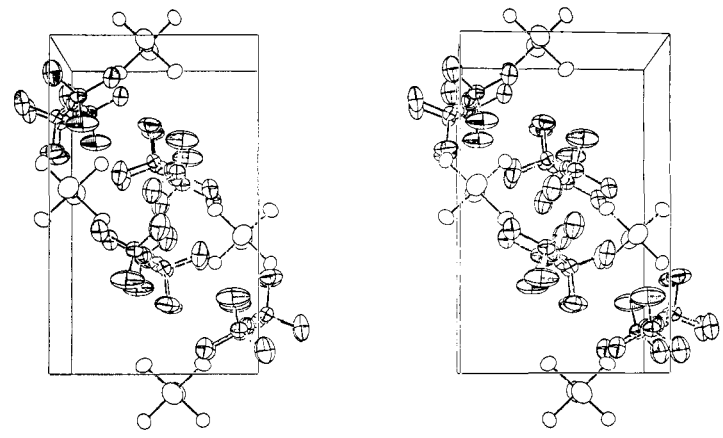

Figure 1. Molecular structures, atomic numbering schemes, and stereo ORTEP views of OP_2NCl_5 (**7**), $OP_3N_2Cl_7$ (**10**), and $P_4N_3Cl_{10}^+PCl_6^-$ (**14**).

It has been speculated[6] that hydrogen bonding involving amino residues could exert a significant influence on the conformation of poly(aminophosphazenes) that bear NHR side groups. However, in **9** no atom is closer than 2.2 Å to the hydrogen atoms attached to the amino nitrogens. In arylaminophosphazenes, hydrogen bonding may be inhibited by the steric bulk of the aromatic residues.

Unlike the situation in compound **8**, the P–N skeletal bonds

Table VIII. Fractional Atomic Positional Parameters for $OP_2N(OC_6H_5)_5$ (**8**)

	x	y	z		x	y	z
P(1)	0.3861 (4)	0.5092 (7)	0.3004 (1)	C(46)	0.4910 (2)	0.2610 (3)	0.2625 (7)
P(2)	0.4002 (4)	0.3668 (7)	0.1768 (1)	C(51)	0.4346 (2)	0.3866 (3)	−0.0541 (5)
N	0.4034 (1)	0.4516 (2)	0.1932 (4)	C(52)	0.4765 (2)	0.4123 (4)	−0.0683 (7)
O	0.4060 (1)	0.5083 (2)	0.4292 (3)	C(53)	0.4854 (3)	0.4557 (5)	−0.1775 (9)
O(1)	0.3337 (1)	0.4961 (2)	0.3016 (3)	C(54)	0.4546 (4)	0.4700 (4)	−0.2669 (8)
O(2)	0.3922 (1)	0.5905 (2)	0.2402 (3)	C(55)	0.4127 (3)	0.4445 (5)	−0.2484 (7)
O(3)	0.3510 (1)	0.3407 (2)	0.1658 (3)	C(56)	0.4027 (2)	0.4012 (4)	−0.1425 (6)
O(4)	0.4181 (1)	0.3137 (2)	0.2862 (3)	H(12)	0.256 (1)	0.455 (2)	0.332 (4)
O(5)	0.4259 (1)	0.3403 (2)	0.0530 (3)	H(13)	0.197 (1)	0.500 (3)	0.486 (4)
C(11)	0.3037 (2)	0.5255 (3)	0.3900 (5)	H(14)	0.221 (1)	0.590 (2)	0.617 (4)
C(12)	0.2624 (3)	0.4941 (3)	0.3871 (6)	H(15)	0.290 (1)	0.641 (2)	0.613 (4)
C(13)	0.2302 (2)	0.5187 (4)	0.4718 (7)	H(16)	0.345 (1)	0.603 (2)	0.483 (4)
C(14)	0.2393 (3)	0.5748 (5)	0.5548 (7)	H(22)	0.420 (1)	0.565 (2)	0.003 (4)
C(15)	0.2799 (4)	0.6072 (4)	0.5570 (7)	H(23)	0.394 (1)	0.619 (2)	−0.178 (4)
C(16)	0.3140 (2)	0.5821 (3)	0.4744 (6)	H(24)	0.329 (1)	0.681 (2)	−0.168 (4)
C(21)	0.3734 (2)	0.6142 (3)	0.1235 (6)	H(25)	0.289 (2)	0.715 (2)	0.015 (4)
C(22)	0.3938 (2)	0.5978 (4)	0.0084 (6)	H(26)	0.320 (1)	0.663 (2)	0.194 (4)
C(23)	0.3759 (3)	0.6273 (5)	−0.1047 (8)	H(32)	0.374 (1)	0.227 (2)	0.015 (4)
C(24)	0.3395 (4)	0.6716 (5)	−0.0986 (9)	H(33)	0.342 (1)	0.112 (2)	0.013 (4)
C(25)	0.3191 (3)	0.6857 (5)	0.0156 (9)	H(34)	0.284 (1)	0.073 (2)	0.155 (4)
C(26)	0.3358 (2)	0.6571 (4)	0.1284 (7)	H(35)	0.257 (1)	0.167 (2)	0.304 (4)
C(31)	0.3345 (2)	0.2666 (3)	0.1626 (5)	H(36)	0.291 (1)	0.288 (2)	0.315 (4)
C(32)	0.3491 (2)	0.2171 (3)	0.0704 (6)	H(42)	0.460 (1)	0.388 (2)	0.460 (4)
C(33)	0.3297 (2)	0.1460 (3)	0.0690 (7)	H(43)	0.530 (1)	0.387 (2)	0.521 (4)
C(34)	0.2979 (3)	0.1266 (4)	0.1557 (7)	H(44)	0.576 (1)	0.298 (2)	0.436 (4)
C(35)	0.2844 (2)	0.1771 (4)	0.2454 (7)	H(45)	0.549 (2)	0.227 (3)	0.256 (5)
C(36)	0.3023 (2)	0.2487 (3)	0.2505 (6)	H(46)	0.475 (2)	0.233 (3)	0.194 (5)
C(41)	0.4635 (2)	0.3119 (3)	0.3217 (5)	H(52)	0.499 (2)	0.397 (3)	−0.007 (5)
C(42)	0.4776 (2)	0.3573 (3)	0.4184 (5)	H(53)	0.511 (3)	0.471 (3)	−0.185 (5)
C(43)	0.5212 (2)	0.3517 (2)	0.4589 (7)	H(54)	0.459 (2)	0.502 (3)	−0.338 (5)
C(44)	0.5492 (2)	0.3017 (4)	0.4015 (7)	H(55)	0.392 (2)	0.455 (3)	−0.309 (5)
C(45)	0.5339 (2)	0.2567 (4)	0.3062 (8)	H(56)	0.378 (2)	0.379 (3)	−0.137 (5)

Table IX. Bond Lengths (Å) and Bond Angles (deg) for $OP_2N(NHC_6H_5)_5$ (**9**)

P(1)–N	1.610 (2)	N(10)–C(11)	1.403 (4)
P(1)–O	1.477 (2)	N(20)–H(20)	0.75 (3)
P(1)–N(10)	1.655 (3)	N(20)–C(21)	1.403 (4)
P(1)–N(20)	1.655 (3)	N(30)–H(30)	0.74 (3)
P(2)–N	1.577 (2)	N(30)–C(31)	1.433 (4)
P(2)–N(30)	1.629 (2)	N(40)–H(40)	0.83 (3)
P(2)–N(40)	1.632 (2)	N(40)–C(41)	1.411 (3)
P(2)–N(50)	1.636 (3)	N(50)–H(50)	0.78 (3)
N(10)–H(10)	0.80 (3)	N(50)–C(51)	1.431 (4)
P(1)–N–P(2)	124.8 (1)	P(1)–N(10)–C(11)	127.4 (2)
N–P(1)–O	117.0 (1)	P(1)–N(20)–C(21)	127.4 (2)
N–P(1)–N(10)	110.1 (1)	P(2)–N(30)–C(31)	122.7 (2)
N–P(1)–N(20)	103.8 (1)	P(2)–N(40)–C(41)	127.6 (2)
O–P(1)–N(10)	109.9 (1)	P(2)–N(50)–C(51)	127.7 (2)
O–P(1)–N(20)	113.2 (1)		
N(10)–P(1)–N(20)	101.6 (1)		
N–P(2)–N(30)	117.7 (1)		
N–P(2)–N(40)	116.9 (1)		
N–P(2)–N(50)	103.9 (1)		
N(30)–P(2)–N(40)	100.1 (1)		
N(30)–P(2)–N(50)	108.6 (1)		
N(40)–P(2)–N(50)	109.5 (1)		

in **9** are nearly equal in length (1.61 and 1.58 Å) and are similar to values found for aminocyclophosphazenes.[18] No separation into "double" and "single" skeletal bonds occurs. Surprisingly, the P–N–P skeletal angle is only 124.8°, perhaps a consequence of the van der Waals attractive forces between adjacent aromatic side units.

(f) $OP(NHPh)_2NP(NHPh)_2NP(NHPh)_3$ (12). Crystals of **12** contained clathrated aniline, which was not removed by two recrystallizations from ethanol–water mixtures. However, the presence of the guest molecules did not appear to influence the conformation of **12**. In the crystal structure, the chain direction of each molecule is approximately parallel to one edge of the unit cell, with sequential chains packed in a head-to-tail fashion. The skeletal conformation is a cis–trans planar arrangement, distorted slightly toward helical geometry (Figure 1). Nitrogen atoms N(1) and N(2) deviate by −0.62 and 0.34 Å, respectively, from the plane defined by the three skeletal phosphorus atoms.

The P–N bond distances range from 1.56 to 1.61 Å (av 1.58 Å) (Tables XI and XII) with the variations being in no way compatible with an alternation of short and long bonds. Thus, the delocalization character detected in the other short chain species is also found in **12**. The bond length variations that do exist can be ascribed to the steric effects of the side groups, and especially to the fact that one terminal phosphorus atom bears two anilino residues and an oxygen atom, rather than three anilino units.

The skeletal bond angles at phosphorus (O–P(1)–N(1) = 121.1°, N(1)–P(2)–N(2) = 122.8°, N(2)–P(3)–NHPh = 108.3 to 115.4°) are comparable to those expected in cyclic phosphazenes. However, the bond angles at nitrogen are wider (130.3° at N(1) and 133.8 at N(2)), again reflecting the variability of the angle at nitrogen according to the presence or absence of ring constrictions or side group interactions.

The bonds between the skeletal phosphorus atoms and the anilino nitrogen atoms have an average length of 1.65 Å, which is typical of the values found for aminocyclophosphazenes.[18]

As can be seen from Figure 2, some of the arylamino groups are nearly coplanar. For example, the dihedral angle between –N(10)Ph and –N(30)Ph is 8.5°, while the corresponding value between –N(20)Ph and –N(60)Ph is 17.9°. No evidence for hydrogen bonding interactions could be found.

Relationship of the X-ray Results to the Structures of $(NPCl_2)_n$, $[NP(OPh)_2]_n$ and $[NP(NHPh)_2]_n$. Several different attempts have been made to solve the structure of poly(dichlorophosphazene) from X-ray fiber data[8,19,20] and by conformational analysis techniques.[9] However, none of these attempts yielded an unam-

(18) Reference 3, Appendix I.

(19) Meyer, K. H.; Lotmar, W.; Pankow, G. W. *Helv. Chim. Acta* **1936**, *19*, 930.

(20) Giglio, E.; Pompa, F.; Ripamonti, A. *J. Polym. Sci.* **1962**, *59*, 293.

Table X. Fractional Atomic Positional Parameters for $OP_2N(NHC_6H_5)_5$ (**9**)

	x	*y*	*z*		*x*	*y*	*z*
P(1)	0.26579 (8)	0.45354 (6)	−0.04010 (6)	C(31)	0.1725 (3)	0.4551 (2)	0.2307 (2)
P(2)	0.27576 (9)	0.61756 (6)	0.16495 (7)	C(32)	0.1073 (4)	0.3425 (3)	0.1570 (3)
N	0.3512 (2)	0.5528 (2)	0.0859 (2)	C(33)	0.1235 (4)	0.2596 (3)	0.1931 (3)
O	0.1070 (2)	0.4294 (2)	−0.0879 (2)	C(34)	0.2059 (4)	0.2885 (3)	0.3009 (3)
N(10)	0.3469 (2)	0.4779 (2)	−0.1281 (2)	C(35)	0.2730 (4)	0.4002 (3)	0.3744 (3)
N(20)	0.3059 (3)	0.3423 (2)	−0.0321 (2)	C(36)	0.2566 (4)	0.4847 (3)	0.3406 (3)
N(30)	0.1518 (2)	0.5419 (2)	0.1952 (2)	C(41)	0.2435 (3)	0.7954 (2)	0.1168 (2)
N(40)	0.1855 (2)	0.6897 (2)	0.1194 (2)	C(42)	0.1608 (3)	0.8647 (2)	0.1198 (3)
N(50)	0.4117 (3)	0.7042 (2)	0.2823 (2)	C(43)	0.2158 (4)	0.9675 (3)	0.1155 (3)
C(11)	0.3397 (3)	0.5571 (2)	−0.1742 (2)	C(44)	0.3516 (4)	1.0024 (3)	0.1095 (3)
C(12)	0.2507 (4)	0.6221 (3)	−0.1565 (3)	C(45)	0.4328 (4)	0.9344 (3)	0.1071 (3)
C(13)	0.2462 (4)	0.6981 (3)	−0.2037 (3)	C(46)	0.3809 (3)	0.8310 (3)	0.1089 (3)
C(14)	0.3280 (4)	0.7112 (3)	−0.2697 (3)	C(51)	0.4046 (4)	0.7797 (2)	0.3855 (3)
C(15)	0.4159 (4)	0.6490 (3)	−0.2874 (3)	C(52)	0.2789 (4)	0.8029 (3)	0.3917 (3)
C(16)	0.4227 (3)	0.5716 (3)	−0.2413 (3)	C(53)	0.2799 (5)	0.8769 (3)	0.4935 (3)
C(21)	0.2381 (3)	0.2283 (2)	−0.1110 (2)	C(54)	0.4002 (6)	0.9261 (3)	0.5861 (3)
C(22)	0.2367 (4)	0.1435 (3)	−0.0737 (3)	C(55)	0.5235 (5)	0.9055 (4)	0.5815 (3)
C(23)	0.1708 (4)	0.0313 (3)	−0.1489 (3)	C(56)	0.5280 (5)	0.8294 (3)	0.4793 (3)
C(24)	0.1046 (5)	0.0013 (3)	−0.2603 (3)	N(1)[a]	0.1626 (6)	0.2533 (4)	0.5462 (3)
C(25)	0.1075 (5)	0.0844 (3)	−0.2976 (3)	C(1)[a]	0.1006 (5)	0.3110 (4)	0.5511 (3)
C(26)	0.1725 (4)	0.1976 (3)	−0.2244 (3)	C(2)[a]	0.0311 (6)	0.3916 (5)	0.5622 (6)
	x	*y*	*z*		*x*	*y*	*z*
H(10)	0.418 (3)	0.459 (2)	−0.124 (2)	H(34)	0.216 (3)	0.232 (2)	0.321 (2)
H(12)	0.198 (3)	0.616 (2)	−0.116 (2)	H(35)	0.326 (3)	0.430 (2)	0.451 (2)
H(13)	0.189 (3)	0.738 (2)	−0.190 (2)	H(36)	0.297 (3)	0.563 (2)	0.392 (2)
H(14)	0.318 (3)	0.759 (2)	−0.297 (2)	H(40)	0.096 (3)	0.669 (2)	0.109 (2)
H(15)	0.465 (3)	0.650 (2)	−0.338 (2)	H(42)	0.070 (3)	0.839 (2)	0.128 (2)
H(16)	0.474 (3)	0.522 (2)	−0.259 (2)	H(43)	0.161 (3)	1.011 (2)	0.122 (2)
H(20)	0.338 (3)	0.352 (2)	0.028 (2)	H(44)	0.387 (3)	1.072 (2)	0.108 (2)
H(22)	0.281 (3)	0.169 (2)	0.005 (2)	H(45)	0.516 (3)	0.953 (2)	0.101 (2)
H(23)	0.170 (3)	−0.026 (2)	−0.121 (2)	H(46)	0.436 (3)	0.786 (2)	0.110 (2)
H(24)	0.062 (3)	−0.069 (2)	−0.308 (2)	H(50)	0.489 (3)	0.700 (2)	0.284 (2)
H(25)	0.063 (3)	0.065 (2)	−0.371 (2)	H(52)	0.191 (3)	0.764 (2)	0.323 (2)
H(26)	0.181 (3)	0.255 (2)	−0.248 (2)	H(53)	0.188 (3)	0.894 (2)	0.500 (2)
H(30)	0.074 (3)	0.531 (2)	0.166 (2)	H(54)	0.394 (3)	0.980 (2)	0.658 (2)
H(32)	0.052 (3)	0.322 (2)	0.084 (2)	H(55)	0.613 (3)	0.919 (2)	0.618 (2)
H(33)	0.069 (3)	0.183 (2)	0.139 (2)	H(56)	0.611 (3)	0.810 (2)	0.464 (2)

[a] Atom designations N(1), C(1), and C(2) for the acetonitrile moleule included in the lattice.

Table XI. Bond Lengths (Å) and Bond Angles (deg) for $OP_3N_2(NHC_6H_5)_7$ (**12**)

P(1)–N(1)	1.58 (1)	N(10)–C(11)	1.40 (2)
P(2)–N(1)	1.57 (1)	N(20)–C(21)	1.38 (2)
P(2)–N(2)	1.61 (1)	N(30)–C(31)	1.45 (2)
P(3)–N(2)	1.56 (1)	N(40)–C(41)	1.44 (2)
P(1)–O	1.493 (9)	N(50)–C(51)	1.42 (1)
P(1)–N(10)	1.67 (2)	N(60)–C(61)	1.42 (2)
P(1)–N(20)	1.67 (1)	N(70)–C(71)	1.47 (2)
P(2)–N(30)	1.65 (1)	N(80)–C(81)	1.31 (3)
P(2)–N(40)	1.66 (1)		
P(3)–N(50)	1.62 (1)		
P(3)–N(60)	1.65 (1)		
P(3)–N(70)	1.62 (2)		
O–P(1)–N(1)	121.2 (6)	N(2)–P(3)–N(50)	108.3 (6)
N(1)–P(1)–N(10)	110.9 (7)	N(2)–P(3)–N(60)	115.4 (6)
N(1)–P(1)–N(20)	101.4 (6)	N(2)–P(3)–N(70)	111.6 (7)
N(10)–P(1)–N(20)	107.3 (6)	N(50)–P(3)–N(60)	102.3 (7)
O–P(1)–N(10)	104.4 (6)	N(50)–P(3)–N(70)	111.0 (6)
O–P(1)–N(20)	111.2 (6)	N(60)–P(3)–N(70)	107.9 (6)
N(1)–P(2)–N(2)	122.8 (7)	P(1)–N(1)–P(2)	130.3 (6)
N(1)–P(2)–N(30)	109.6 (5)	P(2)–N(2)–P(3)	133.8 (7)
N(2)–P(2)–N(30)	100.3 (7)		
N(1)–P(2)–N(40)	105.9 (7)	P(1)–N(10)–C(11)	129.9 (9)
N(2)–P(2)–N(40)	108.4 (6)	P(1)–N(20)–C(21)	130 (1)
N(30)–P(2)–N(40)	109.4 (7)	P(2)–N(30)–C(31)	125 (1)
		P(2)–N(40)–C(41)	127 (1)
		P(2)–N(50)–C(51)	130 (1)
		P(2)–N(60)–C(61)	127 (1)
		P(2)–N(70)–C(71)	130 (1)

biguous structure solution, mainly because the inferred bond angles and lengths drew heavily on data derived from chloro*cyclo*phosphazenes. The data obtained in this present work suggest a different set of primary structural parameters, and these appear to resolve many of the earlier ambiguities.

First, as discussed, it was found that the skeletal P–N bonds in short-chain species **7**, **10**, and **14** are similar in bond length and are not resolved into alternating short and long bonds. This suggests that the same situation exists in poly(dichlorophosphazene) as shown earlier for poly(difluorophosphazene).[7] Thus, the concept of skeletal electron delocalization seems to be as valid for linear phosphazenes as it is for cyclophosphazenes. Although some variation in the value of the P-N bond length was found in species **7**, **10**, and **14** (Tables I, III, and V), it is clear that these linkages have a distinct multiple bond character. Allowing for end-group effects, the combined data from species **7**, **10**, and **14** suggest that the P–N bond length in the $(NPCl_2)_n$ high polymer should be in the range of 1.54–1.55 Å. This is only slightly longer than the value of 1.52 Å determined previously from fiber X-ray data for poly(difluorophosphazene), $(NPF_2)_n$, and is consistent with the slight skeletal bond lengthening expected when the less electronegative chlorine atoms are present.

The average value for the P–Cl bond lengths in the short-chain molecules is 1.95 Å. However, this average includes the somewhat shorter terminal bonds. The average for the PCl_2 middle units in **10** and **14** is 1.98 Å, and this is the value predicted to apply to high polymeric $(NPCl_2)_n$.

The N–P–N bond angles in **10** and **14** are 116.8° and 110.9°, respectively. The interesting result is that both of these values are narrower than the 120° angle previously assumed from the cyclic data. Because the angle in **14** may be affected by the cationic charge, we favor a predicted N–P–N angle near 117° in the $(NPCl_2)_n$ high polymer. On the other hand, the P–N–P angles in the short-chain species vary widely over the range 128.7° to ≃146°, and these values are believed to be a response to relatively small side-group electronic or chain-packing variations.

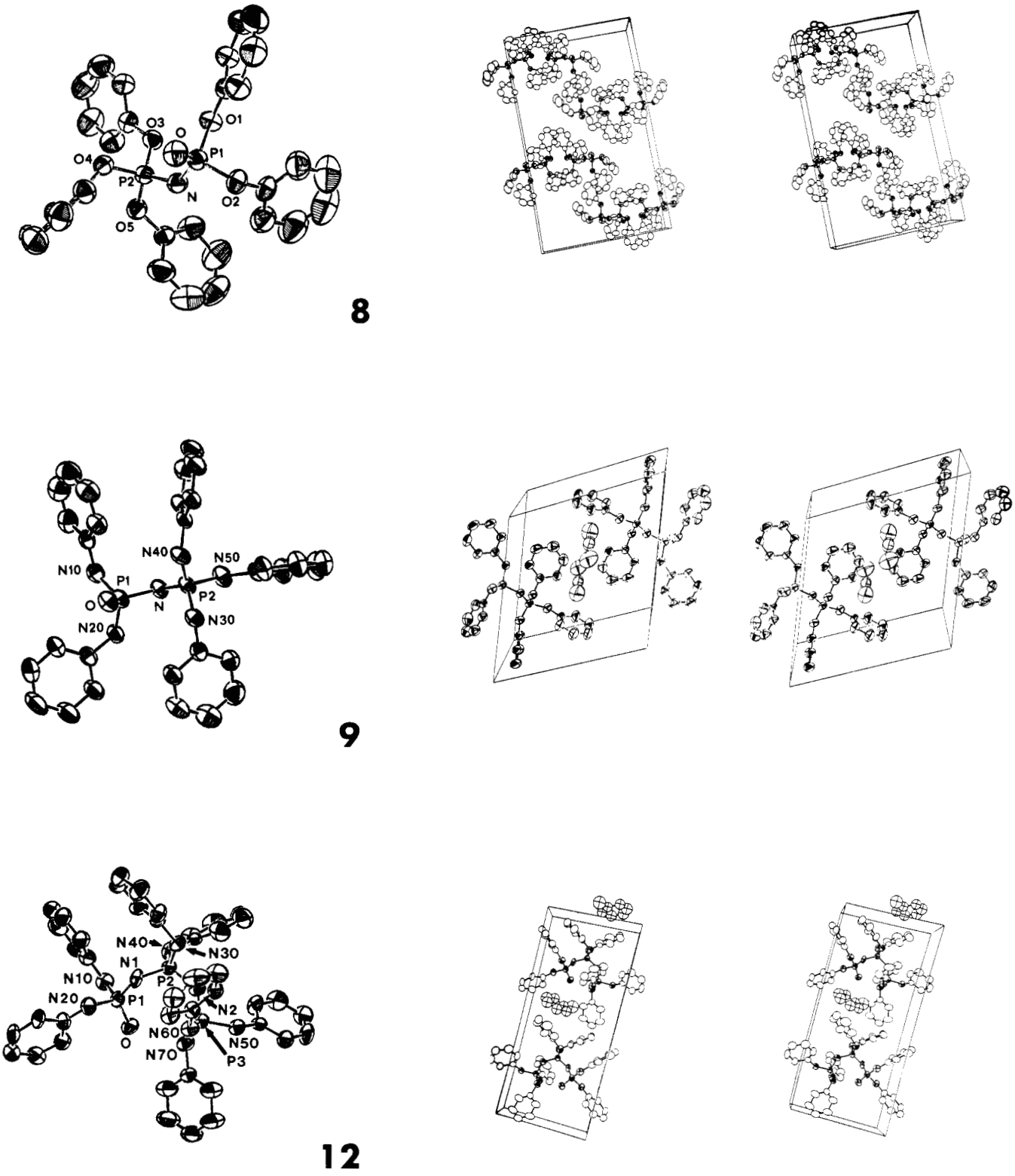

Figure 2. Molecular structures, atomic numbering schemes, and stereo ORTEP views of $OP_2N(OC_6H_5)_5$ (**8**), $OP_2N(NHC_6H_5)_5$ (**9**), and $OP_3N_2(NHC_6H_5)_7$ (**12**).

Thus, although the P–N–P angle in $(NPCl_2)_n$ is now believed to be wider than was previously supposed, its exact value must still be inferred indirectly. However, if a near cis–trans planar chain conformation is assumed for the high polymer, the known repeat distance of 4.92 Å[8,19,20] requires a P–N–P angle in the region of 138°.

The most striking feature of all the short-chain chlorophosphazenes studied in this work is the planarity or near planarity of the phosphazene skeleton. This is perhaps the most convincing evidence found to date that the microcrystalline domains in the high polymer contain planar skeletal sequences. Furthermore, the structure of **10** strongly suggests that the conformation favored by $(NPCl_2)_n$ would be close to cis–trans planar. This reinforces the proposal made several years ago by Giglio, Pompa, and Ripamonti[20] and by ourselves[8,9] and is contrary to the original suggestion by Meyer, Lotmar, and Pankow[19] that the conformation is a spiral helix.

The same arguments apply to the organophosphazene high polymers, $[NP(OPh)_2]_n$ and $[NP(NHPh)_2]_n$. The P–N distances in both of these polymers are estimated from the short-chain analogues to be near 1.59 Å (see the values deduced for **8**, **9**, and **12**), with an N–P–N angle near 123° (see the structure of **12**).

Table XII. Fractional Atomic Positional Parameters for $OP_3N_2(NHC_6H_5)_7$ (**12**)

	x	*y*	*z*		*x*	*y*	*z*
P(1)	0.7986 (4)	0.2500	0.3058 (4)	C(41)	1.020 (1)	0.4054 (6)	0.604 (1)
P(2)	0.7894 (4)	0.3233 (2)	0.5092 (3)	C(42)	1.154 (2)	0.4206 (8)	0.593 (2)
P(3)	0.8612 (4)	0.2261 (2)	0.6939 (3)	C(43)	1.255 (2)	0.4597 (9)	0.688 (3)
O	0.914 (1)	0.2052 (5)	0.3837 (9)	C(44)	1.236 (2)	0.4778 (9)	0.793 (2)
N(1)	0.720 (1)	0.2898 (6)	0.3732 (9)	C(45)	1.105 (2)	0.4636 (9)	0.803 (2)
N(2)	0.862 (1)	0.2905 (5)	0.650 (1)	C(46)	1.004 (2)	0.4238 (8)	0.709 (2)
N(10)	0.886 (1)	0.2905 (6)	0.236 (1)	C(51)	1.065 (1)	0.2458 (6)	0.954 (1)
N(20)	0.649 (1)	0.2193 (6)	0.184 (1)	C(52)	1.119 (2)	0.2233 (8)	1.083 (1)
N(30)	0.656 (1)	0.3619 (5)	0.526 (1)	C(53)	1.251 (2)	0.247 (1)	1.178 (1)
N(40)	0.919 (1)	0.3679 (6)	0.501 (1)	C(54)	1.327 (2)	0.2908 (9)	1.154 (2)
N(50)	0.926 (1)	0.2246 (6)	0.854 (1)	C(55)	1.274 (2)	0.3124 (8)	1.026 (2)
N(60)	0.692 (1)	0.1963 (5)	0.646 (1)	C(56)	1.145 (2)	0.2894 (8)	0.926 (1)
N(70)	0.960 (1)	0.1844 (6)	0.644 (1)	C(61)	0.558 (1)	0.2240 (7)	0.638 (1)
C(11)	0.827 (1)	0.3329 (7)	0.135 (2)	C(62)	0.419 (2)	0.2006 (8)	0.546 (2)
C(12)	0.914 (2)	0.3549 (7)	0.079 (2)	C(63)	0.288 (2)	0.2244 (9)	0.546 (2)
C(13)	0.859 (3)	0.3964 (9)	−0.022 (2)	C(64)	0.292 (2)	0.2677 (8)	0.626 (2)
C(14)	0.711 (3)	0.4159 (8)	−0.063 (2)	C(65)	0.428 (2)	0.2907 (8)	0.714 (2)
C(15)	0.624 (2)	0.3955 (8)	−0.005 (2)	C(66)	0.564 (2)	0.2672 (7)	0.723 (1)
C(16)	0.680 (2)	0.3565 (8)	0.094 (2)	C(71)	1.013 (1)	0.1242 (6)	0.682 (1)
C(21)	0.642 (2)	0.1835 (7)	0.082 (1)	C(72)	1.054 (2)	0.0943 (7)	0.599 (2)
C(22)	0.771 (2)	0.1514 (8)	0.092 (2)	C(73)	1.107 (2)	0.0366 (8)	0.628 (2)
C(23)	0.756 (2)	0.1156 (8)	−0.014 (2)	C(74)	1.115 (2)	0.0125 (8)	0.743 (2)
C(24)	0.626 (3)	0.1088 (9)	−0.125 (2)	C(75)	1.073 (3)	0.0405 (9)	0.822 (2)
C(25)	0.500 (3)	0.1376 (9)	−0.129 (2)	C(76)	1.022 (2)	0.0989 (8)	0.794 (2)
C(26)	0.507 (2)	0.1739 (7)	−0.030 (1)	N(80)[a]	0.338 (3)	0.576 (1)	0.508 (3)
C(31)	0.541 (1)	0.3960 (6)	0.420 (1)	C(81)[a]	0.477 (3)	0.571 (1)	0.601 (2)
C(32)	0.572 (2)	0.4235 (7)	0.327 (2)	C(82)[a]	0.572 (3)	0.546 (2)	0.553 (3)
C(33)	0.454 (2)	0.4556 (8)	0.223 (2)	C(83)[a]	0.726 (3)	0.546 (1)	0.656 (3)
C(34)	0.311 (2)	0.4574 (9)	0.222 (2)	C(84)[a]	0.765 (4)	0.566 (2)	0.778 (3)
C(35)	0.285 (2)	0.4313 (9)	0.316 (2)	C(85)[a]	0.656 (4)	0.587 (2)	0.802 (3)
C(36)	0.398 (2)	0.3980 (7)	0.417 (1)	C(86)[a]	0.503 (3)	0.595 (1)	0.721 (3)

[a] Atom designations for the aniline molecule included in the lattice.

Table XIII. ^{31}P NMR Assignments[a]

compound	chemical shift (ppm)[b]	coupling constant *J* (Hz)
$(NPCl_2)_3$	+19.9	
$(NPCl_2)_n$	−17.4[c]	
OP_2NCl_5 (**7**)	A, −12.0; B, −4.1	J_{AB} = 19.5
$OP_3N_2Cl_7$ (**10**)	A, −11.4; B, −19.2; C, +6.8	J_{AB} = 28.5; J_{BC} = 29.0
$OP_4N_3Cl_9$ (**13**)	A, −11.5; B, −20.5; C, −15.9; D, +6.4	J_{AB} = 28.2; J_{BC} = 39.0; J_{CD} = 33.2; J_{CA} = 5.1; J_{BD} = 4.7
$OP_5N_4Cl_{11}$ (**15**)	A, −12.3; B, −22.2; C, −17.4; D, −15.4; E, +7.5	J_{AB} = 28.0; J_{BC} = 29.3; J_{CB} = 38.7; J_{CD} = 31.1; J_{ED} = 32.9; (J_{AC} < 8); J_{BD} = 6.3; (J_{CE} < 4)
$OP_6N_5Cl_{13}$ (**16**)	A, −11.2; B, −21.9; C, −17.9; D, −15.8; E, −14.4; F, +8.3	J_{AB} = 34.9; J_{BC} = 39.7; J_{CD} = 40.6; J_{DE} = 38.9; J_{EF} = 33.9
$[NP(OPh)_2]_3$	+8	
$[NP(OPh)_2]_n$	−18.7	
$OP_2N(OPh)_5$ (**8**)	A, −22.7; B, −15.18	J_{AB} = 75.80
$OP_3N_2(OPh)_7$ (**11**)	A, −23.44; B, −19.08; C, −14.46	J_{AB} = 71.23; J_{BC} = 66.65; J_{AC} = 7.30
$[NP(NHC_6H_5)_2]_3$	+2	
$[NP(NHC_6H_5)_2]_n$	−14.0	
$OP_2N(NHC_6H_5)_5$ (**9**)	A, −10.96; B, −7.77	J_{AB} = 50.7
$OP_3N_2(NHC_6H_5)_7$ (**12**)	A, −10.7; B, −15.4; C, −5.8	J_{AB} = 55.2; J_{BC} = 40.8
$[NP(NHMe_2]_3$	+14.6	
$[NP(NHMe)_2]_n$	+8.7	
$OP_2N(NHMe)_5$	A, +13.7; B, +19.2	J_{AB} = 33.7
$OP_3N_2(NHMe)_7$	A, +13.0; B, +8.6; C, +18.6	J_{AB} = 23.0; J_{BC} = 41.1
$[NP(NMe_2)_2]_3$	+25	
$[NP(NMe_2)_2]_n$	−5	
$OP_2N(NMe_2)_5$	A, +10.9; B, +20.4	J_{AB} = 47.5
$OP_3N_2(NMe_2)_7$	A, +11.9; B, +2.7; C, +16.3	J_{AB} = 42.4; J_{BC} = 53.1

[a] The phosphorus atom designations are the following: atom A bears the terminal oxygen atom; atom B is the next one along the chain; etc. [b] In $CDCl_3$. [c] In THF.

For $[NP(OPh)_2]_n$, the chain repeat distance is 4.91 Å.[5,21] If a cis–trans planar conformation is assumed for this polymer, the P–N–P angle is calculated to be near 124°. The chain repeat distance for $[NP(NHPh)_2]_n$ is not known.

The structures of **8**, **9**, and **12** are also compatible with the idea that, in the high polymeric analogues, the aromatic side groups play a significant role in stabilizing the skeletal conformation. Therefore, it seems likely that these same forces would discourage conformational mobility, and this may explain the rather high glass transition values found for $[NP(OPh)_2]_n$ (+55 °C) and $[NP(NHPh)_2]_n$ (+91 °C), compared to the low values found for $(NPCl_2)_n$ (−63 °C) and $(NPF_2)_n$ (−96 °C).[4-7]

Relationship of the ^{31}P NMR Spectra of the Short-Chain Species to Spectra of the High Polymers. A broader range of short-chain models could be studied by ^{31}P NMR techniques than by X-ray diffraction. Thus, the spectra of **7**–**16** were examined and compared with the related cyclic trimers and tetramers. The chemical shifts are listed in Table XIII.

(21) Allcock, H. R.; Stroh, E. G., unpublished results.

The ^{31}P spectra are important because they provide information about skeletal bond torsional mobility and about the effect of chain length and end-group character on the electronic structure of the backbone. For example, ^{31}P NMR shifts are sensitive to the π-bond symmetry around phosphorus.[22] Bond torsion would improve π-bond symmetry and increase the shielding, with a corresponding upfield shift of the resonance. Conversely, restriction of torsion by, for example, incorporation of the phosphorus into a ring will generate marked downfield shifts compared to the situation in flexible, linear molecules. Bulky substituent groups attached to a chain would inhibit torsion and give the same effect.

For the chlorophosphazenes, **7**, **10**, **13**, **15**, and **16**, the end groups yielded doublets from nuclear spin–spin coupling to the nearest phosphorus in the backbone. The $-PCl_3$ end group was always furthest downfield, in the region of −4.0 to +7.5 ppm, and was always broadened relative to the other resonances. The $O{=}PCl_2-$ end groups yielded a set of resonances (a doublet or, where coupling to a once-removed phosphorus was found, a doublet of doublets) immediately upfield from $-PCl_3$. The $O{=}PCl_2-$ resonance was relatively unaffected by chain length and occurred at approximately −12 ppm in all five linear chlorophosphazenes.

The $NPCl_2$ middle units in **10** and **13**–**16** gave resonances in the −15 to −20 ppm region. This can be compared with the value of −17.4 ppm found for the $(NPCl_2)_n$ high polymer, and the values of +19.7 and +7.4 ppm found for the cyclic oligomers $(NPCl_2)_3$ and $(NPCl_2)_4$. The $-NPCl_2-$ resonances in the short chains, expected as doublets of doublets, generally appeared as triplets. Accidental overlapping of these resonances produced more complex patterns, as in the spectra of **15** and **16**. Coupling constants were in the region of 28–40 Hz.

Even when only three phosphorus atoms are present in the chain (**10**), the character of the spectrum more closely resembles that of the linear high polymer than of the cyclic trimer. In compounds **15** and **16** some of the phosphorus resonances overlap. The spectrum of poly(dichlorophosphazene) is the logical extension of the trends evident in the short-chain species. In the polymer each phosphorus atom is indistinguishable from its neighbors, and the ^{31}P NMR spectrum consists of a sharp singlet. No end groups can be detected in the polymer, which may be a consequence of the extremely long chain length or the presence of macrocyclic structures.

These trends are also evident for the short-chain organophosphazenes, **8**, **9**, **11**, **12**, and for the additional derivatives $O{=}P(NHMe)_2NP(NHMe)_3$, $O{=}P(NHMe)_2NP(NHMe)_2NP(NHMe)_3$, $O{=}P(NMe_2)_2NP(NMe_2)_3$, and $O{=}P(NMe_2)_2NP(NMe_2)_2NP(NMe_2)_3$ (Table XIII). With the exception of the phosphorus–phosphorus coupling, the end groups have very little influence on the $-NPR_2-$ resonance. Pronounced similarities exist between the chemical shift positions of the $-NPR_2-$ resonances in the short-chain species and in the analogous high polymers, and these differ markedly from the chemical shifts of the cyclic trimers.

Experimental Section

Materials. Diethyl ether, tetrahydrofuran (THF), and dioxane (Baker) were distilled under nitrogen from sodium benzophenone ketyl. Methylene chloride was distilled from CaH_2. Phosphorus pentachloride, phosphorus oxychloride, sodium hydride (60% dispersion in mineral oil), phenol, and 1,1,1,3,3,3-hexamethyldisilazane (Aldrich) were used as received. Ammonium sulfate was dried at 120 °C for 24 h and stored under nitrogen. Aniline (Aldrich) was vacuum distilled from KOH and stored under nitrogen in the absence of light. Methylamine and dimethylamine (Matheson) were dried with sodium/potassium alloy and benzophenone in the condensed phase before use. *sym*-Tetrachloroethane was purified by the method described by Weissberger et al.[23]

Synthesis of the Phosphazenes. OP_2NCl_5 (7). Compound **7** was synthesized from PCl_5 (187 g, 0.90 mol) and $(NH_4)_2SO_4$ (26.4 g, 0.20 mol) in *sym*-tetrachloroethane (*s*-TCE) (≃ 400 mL) by the method of Emsley, Moore, and Udy[12] and was purified by vacuum distillation twice. It was obtained as colorless crystals.

$OP_3N_2Cl_7$ (10). Species **10** was synthesized by the method of Riesel.[13] Specifically, $NHSi_2(CH_3)_6$ (40 mL, 0.190 mol) in CH_2Cl_2 (50 mL) was added dropwise to **7** (50 g, 0.187 mol) in CH_2Cl_2 (200 mL). The reaction mixture was refluxed for 10–12 h. PCl_5 (40 g, 0.194 mol) was added via a Schlenk addition tube, and the reaction mixture was refluxed for an additional 12 h. The solvent was removed by rotoevaporation and the product, **10**, was purified twice by vacuum distillation (170–175 °C (0.1 mmHg)). Compound **10** was obtained as colorless crystals.

$OP_4N_3Cl_9$ (13). Species **13** was synthesized by passing SO_2(g) over the ionic species $P_4N_3Cl_{10}^+Cl^-$ or $P_4N_3Cl_{10}^+PCl_6^-$.[14] Volatile side products were removed in vacuo. Because **13** could not be purified without decomposition, it was isolated as an impure, colorless oil. The impurities (<10%) were detected by ^{31}P NMR spectroscopy.

$OP_5N_4Cl_{11}$ (15) and $OP_6N_5Cl_{13}$ (16). Compounds **15** and **16** were prepared by the same general procedure. $OPCl_3$ (for **15**) or OP_2NCl_5 (for **16**) was treated with 1 molar equiv of $NHSi_2(CH_3)_6$ in CH_2Cl_2 (≃200 mL). The reaction mixture was heated at reflux for 10–12 h. $P_4N_3Cl_{10}^+Cl^-$ (1.1–1.2 molar equiv) was added via a Schlenk addition tube, and the reaction mixture was refluxed for another 10–12 h. The solvent was then removed. Species **15** and **16** were obtained as pale brown oils. They were characterized by ^{31}P NMR spectroscopy (Table XIII) and by mass spectrometry.[24]

Reactions of 7 and 10 with Nucleophiles. Reaction with Sodium Phenoxide. Sodium phenoxide (3–4 molar equiv per P–Cl) was prepared from excess sodium hydride and phenol in dioxane. Phosphazene **7** or **10** (≃5–8 mmol) in dioxane (50 mL) was added dropwise to the phenoxide solution. The reaction mixture was stirred at room temperature for 3 days. It was then filtered through silica and passed down a short silica column. Removal of the solvent gave $OP_2N(OPh)_5$ as needles and $OP_3N_2(OPh)_7$ as a colorless oil. $OP_2N(OPh)_5$ was purified further by recrystallization from isopropyl ether/hexane mixtures. Both organophosphazenes were characterized by ^{31}P NMR spectroscopy and mass spectrometry.[24]

Reaction with Aniline. The phosphazene **7** or **10** in diethyl ether (50 mL) was added dropwise to aniline (≃4 molar equiv per P–Cl) in diethyl ether (50 mL) chilled with ice/water. The reaction mixture was stirred for 3 days, and the solvent was then removed by rotoevaporation. Ethanol (≃30 mL) was added, the solution was filtered, and distilled water was added until moderate turbidity was observed. After several days, white, needlelike crystals of $OP_2N(NHPh)_5$ or $OP_3N_2(NHPh)_7$ formed. These compounds were purified by recrystallization, $OP_2N(NHPh)_5$ from acetonitrile, and $OP_3N_2(NHPh)_7$ from ethanol/water. Both compounds were characterized by ^{31}P NMR spectroscopy and mass spectrometry.[24]

Reaction with Monomethylamine or Dimethylamine. The amine CH_3NH_2 or $(CH_3)_2NH$ was condensed over Na/K-benzophenone. This was recondensed into a reaction vessel charged with diethyl ether (50 mL) and was maintained at reduced temperature with ice/water. The reaction vessel was equipped with a dry ice condenser to return gaseous amine to the reaction solution. The phosphazene **7** or **10** in diethyl ether (25 mL) was added dropwise to the amine. The reduced temperature was maintained for 2 h, after which time the excess amine was allowed to evaporate. The amino-substituted phosphazenes were isolated by extraction with dichloromethane. Removal of the solvent yielded $OP_2N(NHCH_3)_5$, $OP_3N_2(NHCH_3)_7$, $OP_2N(N(CH_3)_2)_5$, or $OP_3N_2(N(CH_3)_2)_7$. These were characterized by ^{31}P NMR spectroscopy and mass spectrometry.[24] They were obtained as pale yellow oils. The microanalytical data for the organophosphazenes are listed in the Supplementary Material.

X-ray Structure Determination. Crystal Preparations. Crystals of OP_2NCl_5 (**7**) and $OP_3N_2Cl_7$ (**10**) were prepared as follows: Single crystals were grown at room temperature from the melt under an inert atomsphere. Crystals 0.3–0.5 mm in the shortest direction were selected and manipulated in a drybox. The crystals were mounted in borosilicate glass capillaries which were sealed with epoxy cement. Crystals of $P_4N_3Cl_{10}^+PCl_6^-$ (**14**) were dissolved in CH_2Cl_2 under an inert atmosphere, and recrystallization was induced by slow cooling. Suitable crystals were mounted in borosilicate capillaries. $OP_2N(OPh)_5$ (**8**) was dissolved in isopropyl ether/hexane mixtures, and crystals suitable for structural analysis were obtained by slow cooling of the solution. A crystal was mounted on a glass fiber with epoxy cement. $OP_2N(NHPh)_5$ (**9**) was recrystallized from acetonitrile solution at room temperature. Individual crystals were mounted in borosilicate capillaries to prevent loss of included solvent. Crystals of $OP_3N_2(NHPh)_7$ (**12**) were obtained from ethanol/water at room temperature, and a selected crystal was mounted

(22) Crutchfield, M. M.; Dungan, C. H.; Letcher, J. H.; Mark, V.; Van Wazer, J. R. "^{31}P Nuclear Magnetic Resonance" In "Topics in Phosphorus Chemistry"; Grayson, M., Griffith, E. J., Eds.; Interscience: New York, 1967; Vol. 5.

(23) Weissberger, A. "Technique of Organic Chemistry"; Interscience: New York, 1967; Vol. III.

(24) Parent ion peaks were detected plus molecular fragments that corresponded to a loss of one to four substituents attached to phosphorus.

Table XIV. Summary of Crystal Data and Intensity Collection Parameters

	OP_2NCl_5[a] (7)	$OP_3N_2Cl_7$ (10)	$P_4N_3Cl_{10}^+PCl_6^-$ (14)	$OP_2N(OPh)_5$ (8)	$OP_2N(NHPh)_5$ (9)	$OP_3N_2(NHPh)_7$ (12)
fw, amu	269.22	385.11	764.14	557.48	593.61	874.91
space group	$P2_1/n$	$P\bar{1}$	*Pnam*	*Pbca*	$P\bar{1}$	$P2_1$
a, Å	8.050 (1)	6.087 (4)	10.402 (2)	30.108 (7)	10.006 (4)	9.762 (2)
b, Å	19.562 (2)	8.566 (3)	17.482 (2)	17.834 (4)	13.336	22.912 (4)
c, Å	11.392 (2)	12.561 (5)	13.804 (2)	10.303 (2)	13.390 (3)	11.156 (4)
α, deg		106.66 (3)			110.12 (2)	
β, deg	102.35 (1)	90.40 (4)			103.50 (3)	115.50 (3)
γ, deg		94.70 (5)			103.49 (3)	
vol, Å^3	1752 (1)	625 (1)	2510 (1)	5532 (3)	1532 (2)	2252 (2)
Z	8	2	4	8	2	2
d(calcd), g/cm^3	2.041	2.046	2.020	1.339	1.286	1.290
crystal dim, mm	0.45 × 0.45 × 0.55	0.32 × 0.42 × 0.46	0.31 × 0.36 × 0.57	0.15 × 0.17 × 0.38	0.16 × 0.23 × 0.51	0.17 × 0.29 × 0.33
A	1.00	1.25	0.85	0.6	1.0	0.8
background	0.5	0.5	0.5	0.5	0.5	0.5
2θ limits, deg	3.2–41.6	2.8–41.8	3.2–51.4	3.0–46.4	3.2–45.74	3.2–56.16
unique obsd data	1575	1178	1482 ($I > 3\sigma(I)$)	2915	2755	2644
ρ	0.05	1.0	1.0	1.0	0.04	1.0
μ, cm^{-1}	19.6	19.5	20.8	2.07	1.74	1.75
R/R_w	0.071/0.065	0.094/0.114	0.066/0.066	0.046/0.046	0.041/0.046	0.089/0.088
esd	2.802	2.957	3.136	2.017	1.384	2.586
data/param.	9.97	9.98	12.56	6.83	5.76	5.06
drift corr[b]		1.000–1.007	0.994–1.000		1.000–1.003	0.999–1.000
drift corr[c]	0.965–1.000	0.949–1.599	0.981–1.090	0.833–1.044	0.907–1.018	0.961–1.070
largest residual peak, e$^-$ Å^{-3}	1.27	0.90	0.72	0.18	0.19	0.69

[a] These values are for the data set collected at −50 °C. [b] Empirical. [c] Anisotropic.

on a glass fiber with epoxy cement.

Data Collection and Reduction. A given crystal was optically centered on an Enraf-Nonius four-circle CAD4 automated diffractometer controlled by a PDP8/a computer coupled to a PDP11/34 or 11/44 computer. A full rotation orientation photograph was taken with a Polaroid cassette accessory, and 25 reflections were chosen and centered with the use of manufacture-supplied software. The INDEX program was used to obtain an orientation matrix and unit cell parameters. Successive centerings and least-square refinements of 2θ values found for the 25 precisely centered reflections gave the lattice constants listed in Table XIV for each of the 6 crystals. A small test data set (axial and zero-layer reflections) was collected to determine systematic absences and choice of space group.

Intensity data were collected at room temperature or −50 °C with a graphite single crystal monochromator using Mo Kα radiation (λ = 0.71073 Å; takeoff angle 2.8°). A θ–2θ mode was used with 2θ ranging from $(A + 0.347 \tan \theta)°$ below the calculated position of the Kα reflection to $(A + 0.347 \tan \theta)°$ above the calculated position of the Kα reflection. The *A* values are given in Table XIV. The scan rate was varied automatically from 1° to 5° min^{-1}, depending on the intensity of a reflection as determined by a preliminary brief scan. Three standard reflections were measured after every hour and were recentered after every 200 reflections to check crystal orientation and stability. The total number of unique reflections observed in each case is given in Table XIV, with the criterion for observations being $I > 2\sigma(I)$ unless otherwise noted.

Linear absorption coefficients for Mo Kα radiation are also given in Table XIV. The values were sufficiently small that no absorption corrections were applied. The data were processed by manufacturer-supplied software. The integrated intensity, *I*, was calculated according to the expression $I = [Sc - 2(B_1 + B_2)]T_r$, where Sc is the count accumulated during the scan, B_1 and B_2 are the background counts at each end of the scan, and T_r is the 2θ scan rate in degrees per minute. $\sigma(I)$ was calculated as follows: $\sigma(I) = T_r[Sc + 4(B_1 + B_2) + (\rho I)^2]^{1/2}$, where ρ values are indicated in Table XIV.

In all cases, the standard reflections were used to rescale the data automatically to correct for drift due to changes in temperature, centering, etc. The unique, normalized, integrated intensity set was processed to give *F* and *E* values. Polarization corrections were calculated from the assumption that the incident beam is polarized to some extent by the monochromator. The graphite crystal was assumed to be 50% perfect and 50% mosaic for this purpose.

All the structure solutions were initiated through the use of direct methods and, where feasible, these were checked by the use of Patterson syntheses. All non-hydrogen atoms in the phosphorylphosphazenes were located by least-squares analysis and difference Fourier synthesis. In $OP_2N(OPh)_5$ and $OP_2N(NHPh)_5$, the hydrogen atoms were located and refined isotropically. In $OP_3N_2(NHPh)_7$, hydrogen atoms were placed in calculated positions and were unrefined. The non-phosphazene molecules included in the crystalline lattice of $OP_2N(NHPh)_5$ and $OP_3(NHPh)_7$ were located and refined isotropically. The form of the isotropic thermal parameter is $-B \sin^2 \theta/\lambda^2$. Tables of observed and calculated structure factors, thermal parameters, and root mean square amplitudes of thermal vibration for compounds **7**–**10**, **12**, and **14** are given in the Supplementary Material as Tables XVI–XXXIX.

Acknowledgment. This work was supported by the U.S. Army Research Office through Grant No. DAAG2982-K-0045. The X-ray diffraction data and structure solutions were obtained with the use of equipment provided through DOD equipment Grant No. DAAG29-83-G0101.

Registry No. 7, 13966-08-0; **8**, 15241-20-0; **9**, 97150-00-0; **10**, 36778-94-6; **11**, 97149-95-6; **12**, 97150-01-1; **13**, 36775-73-2; **14**, 21246-63-9; **15**, 81005-15-4; **16**, 97149-96-7; $OP_2N(NHCH_3)_5$, 97149-97-8; $OP_3N_2(NHCH_3)_7$, 97149-98-9; $OP_2N(N(CH_3)_2)_5$, 91241-12-2; $OP_3N_2(N(CH_3)_2)_7$, 97149-99-0; $P_4N_3Cl^+Cl^-$, 97170-39-3; NH_4Cl, 12125-02-9; $OPCl_3$, 10025-87-3; $NHSi_2(CH_3)_6$, 999-97-3; CH_3NH_2, 74-89-5; $(CH_3)_2(NH)$, 124-40-3; PCl_5, 10026-13-8; sodium phenoxide, 139-02-6; aniline, 62-53-3.

Supplementary Material Available: Tables of microanalytical characterization data for organophosphorylphosphazenes; anisotropic thermal parameters, root mean square amplitudes of thermal vibration, and values of F_o and F_c for **7**, **8**, **9**, **10**, **12**, and **14**; bond lengths and angles for **7**; fractional atomic positional parameters for **7**; and torsional angles for **7** (94 pages). Ordering information is given on any current masthead page.